JOURNALS OF CATALYSIS **159,** 69–82 (1996)
ARTICLE NO. 0065

Infrared Study of the Adsorption and Reaction of Methyl Chloride and Methyl Iodide on Silica-Supported Pt Catalysts

K. C. McGee, M. D. Driessen, and V. H. Grassian[1]

Department of Chemistry, University of Iowa, Iowa City, Iowa, 52242

Received April 5, 1995; revised November 13, 1995; accepted November 30, 1995

The low-temperature adsorption of methyl chloride and methyl iodide on silica-supported Pt catalysts has been investigated by transmission Fourier transform infrared spectroscopy. The IR data show that methyl chloride and methyl iodide dissociate at low temperatures (near 200 K) to form an adsorbed hydrocarbon fragment on the surface, identified as methyl groups. Methyl groups are characterized by a single infrared absorption band near 2965 cm^{-1}. Methyl groups react with hydrogen to form gas-phase methane as the sample is warmed between 200 and 473 K. Reaction of approximately 10 Torr of methyl chloride at 473 K over a Pt/SiO_2 catalyst shows that only 20% of the methyl chloride decomposes to form gas-phase methane and hydrogen chloride in the absence of hydrogen. However, in the presence of an equal amount of hydrogen, all of the methyl chloride is converted to methane and hydrogen chloride. In contrast to the quantitative conversion of methyl chloride, less than 10% of the initial 10 Torr of methyl iodide forms methane at 473 K and no hydrogen iodide forms in the presence or absence of hydrogen gas. Although the activation barrier for C–Cl bond dissociation in adsorbed methyl chloride is higher than the barrier for C–I bond dissociation in adsorbed methyl iodide, the lower energy barrier for removal of adsorbed chlorine compared to adsorbed iodine is the cause of the higher catalytic activity of Pt/SiO_2 toward methyl chloride decomposition. In addition to the thermal decomposition of CH_3Cl, we have investigated the possibility of using solar radiation for the decomposition of CH_3Cl on Pt/SiO_2. The results for the photo-assisted decomposition of CH_3Cl adsorbed on Pt/SiO_2 are presented and discussed.

INTRODUCTION

In recent years, there have been many studies of alkyl halide adsorption on single-crystal metal surfaces under ultrahigh vacuum conditions (1, 2). Alkyl halides can thermally or photochemically dissociate on metals to form adsorbed alkyl fragments. For example adsorbed methyl groups can be prepared from the dissociation of CH_3X (X = Cl, Br, or I) (3–10):

$$CH_3X(a) \xrightarrow[\text{metal surface}]{h\nu \text{ or } \Delta} CH_3(a) + X(a). \qquad [1]$$

[1] To whom correspondence should be addressed. E-mail: vicki-grassian@uiowa.edu.

Gaining insight into heterogeneous catalysis, through ultrahigh vacuum studies on single-crystal metal surfaces, is a primary goal of surface science (11). One question is how do studies of hydrocarbon fragments formed at 10^{-10} Torr pressure on clean low Miller index single-crystal surfaces provide useful models for reactions that occur at high pressures and on surfaces of more complex structure and composition as is the case for heterogeneous catalysts. Typically, surface science studies involve model reactions on model surfaces, whereas catalysis involves complicated reactions on complex surfaces.

In this study, several questions are addressed. First, how do hydrocarbon fragments, in particular the simplest fragment–methyl, bond to surfaces with more complex structure than single crystal surfaces? Second, supported by recent suggestions that Pt catalysts should be effective toward the decomposition of chlorinated hydrocarbons, (12), can silica-supported Pt catalysts be effective in the decomposition of methyl halides? Third, what is the mechanism for the thermal decomposition of methyl halides on silica-supported Pt catalysts? Fourth, can solar radiation be used to decompose chlorinated hydrocarbons, in particular CH_3Cl, adsorbed on Pt/SiO_2 catalysts? Infrared spectroscopy is used to identify surface-bound species and gas-phase products in the thermal decomposition of CH_3Cl and CH_3I adsorbed on Pt/SiO_2 and in the photo-assisted decomposition of CH_3Cl adsorbed on Pt/SiO_2.

METHODS

Two different IR cells were used in these studies. Both have been described previously (13, 14). For the experiments that involve low temperature adsorption (near 200 K), the IR cell consists of a 1-in.-thick, 2.75-in.-diameter, double-sided conflat flange with two CaF_2 viewports (15). A 1-in.-CaF_2 plate with a uniform layer of the sample is placed in a Cu block assembly. The sample temperature can be varied from approximately 100 to 500 K by circulating cooled or heated nitrogen gas through the copper block. The temperature of the sample is measured with a thermocouple wire placed in direct contact with the CaF_2

0021-9517/96 $18.00

plate. For the experiments that did not involve low temperature adsorption, the sample is sprayed onto a W grid (16). The W grid can be resistively heated for high-temperature experiments (17).

The procedure for preparing the Pt/SiO_2 catalysts includes two steps: wet impregnation, and chemical processing. H_2PtCl_6 (Johnson Matthey) and silica (Cabosil M-5, 200 $m^2\ g^{-1}$) are used to prepare Pt/SiO_2 and SiO_2 samples. Samples are made by spraying a slurry of platinum salt/silica suspended in acetone onto a CaF_2 plate (Harshaw) or photoetched W grid (Bucksbee). In between applications, the slurry is kept homogeneously mixed by placing the solution in an ultrasonic cleaner. The CaF_2 plate or W grid is held on an aluminum template maintained at 333 K. A fine mist from the atomizer hits the CaF_2 plate (W grid) and the acetone flash evaporates, producing a uniform layer of metal salt/support. A template is used to mask half of the sample, allowing one side to be coated with the Pt/SiO_2 and the other side with SiO_2 only. In some experiments, one side was made with either just Pt/SiO_2 or SiO_2 and the other side was left blank in order to monitor gas-phase products. Approximately 10 mg were deposited on each half of the CaF_2 plate. To aid in the spectroscopic detection of surface-bound intermediates, high metal loadings on the order of 15% were used in these experiments.

After the sample is prepared it is mounted inside the IR cell. The IR cell is wrapped in heating tape and baked-out at 473 K for 12–24 h under vacuum. Hydrogen reduction of the metal salt is then done at 473 K for 15 min followed by evacuation for the same period of time. This process is sequentially repeated for 30, 60, and 120 min. H_2 reduction is followed by oxidation with O_2 at 473 K and a pressure of 1.5 Torr. The sample is then reduced again at 473 K.

The IR cell is attached to the vacuum chamber through a stainless steel bellows hose approximately 2 ft. in length with an inner diameter of approximately 1 in. The stainless steel high vacuum apparatus consists of a 20 liter/s ion pump, two absolute pressure transducers, for accurate pressure measurements in the range 0.001–1000 Torr, and an ion gauge. A turbomolecular pump is used to rough-pump the vacuum chamber and to evacuate the gas manifold line used for sample introduction. Following bake-out, the apparatus reaches a base pressure of $<1 \times 10^{-8}$ Torr.

The Pt/SiO_2 catalysts were characterized using several methods. Particle size distributions were determined using scanning transmission electron microscopy (TEM). The micrographs were obtained with a Hitachi H-600 electron microscope operated at an acceleration voltage of 100 kV. For these Pt/SiO_2 samples, the average diameter of the particles was 2 nm. IR spectroscopy of CO was also used to determine if the sample was fully reduced. After the last reduction of the catalyst, CO was adsorbed on the surface. The infrared spectrum showed there were no absorption bands in the infrared that could be associated with oxidized sites, these bands would have frequencies greater than 2100 cm^{-1} (18).

After sample processing, the IR cell is placed on a linear translator inside the spectrometer sample compartment. Either the SiO_2 or the Pt/SiO_2 half of the sample can be translated into the IR beam for data acquisition. This half sample method developed by Yates and co-workers (15, 16) enables the chemistry of both Pt/SiO_2 and SiO_2 to be monitored simultaneously during the course of a particular experiment. For samples that contain Pt/SiO_2 and a blank half, the chemistry of the adsorbed and gas-phase molecules could be monitored.

Infrared measurements are made using a Galaxy 6021 FT-IR spectrometer (Mattson Instruments) with a narrowband MCT detector; 1000 scans are taken with an instrument resolution of 4 cm^{-1}. Absorbance spectra shown represent sample single beam spectra referenced to background single beam spectra recorded for the freshly prepared sample, i.e., either SiO_2 or Pt/SiO_2 prior to reaction. For the temperature-dependent infrared spectra, the sample was warmed to the desired temperature and held there for 30 s before a spectrum was recorded.

Methyl chloride (Mattheson, 99.5%) is used without further purification. Methyl iodide (Aldrich, 99.5%) is stored at 277 K in the dark and subject to several freeze–pump–thaw cycles prior to use. H_2 (99.9995% purity) and O_2 (99.6%) from Air Products were used without further purification.

RESULTS

CH_3Cl and CH_3I Adsorption on Pt/SiO_2 and SiO_2 at Low Temperatures

The IR spectra of CH_3Cl in the gas phase and adsorbed on SiO_2 and Pt/SiO_2 at 205 K, in the presence of an equilibrium pressure of gas-phase CH_3Cl, are shown in Fig. 1. The top spectrum in Fig. 1 shows the gas-phase spectrum obtained at a pressure of 7.1 Torr. The other two spectra shown in Fig. 1 are of CH_3Cl adsorbed on SiO_2 and Pt/SiO_2, at an equilibrium pressure of 7.1 Torr. Gas-phase contributions to the adsorbate spectra have been subtracted out. As can be seen in Fig. 1, there are two distinct regions in the Pt/SiO_2 and SiO_2 spectra: the spectral region above 3200 cm^{-1}, assigned to surface hydroxyl groups on the silica support, and the spectral region between 1300 and 3100 cm^{-1}, assigned to absorption bands due to adsorbed CH_3Cl. The spectral region below 1300 cm^{-1} (not shown) is opaque due to strong absorption by the silica substrate and the CaF_2 plate to which the sample is mounted. For CH_3Cl adsorption on Pt/SiO_2 and SiO_2, the data clearly show that CH_3Cl adsorbs on the silica surface through the surface hydroxyl groups. The negative feature at 3747 cm^{-1} is due to the loss of isolated hydroxyl groups. The positive broad feature at lower frequency near 3604 cm^{-1} is a result of hydrogen

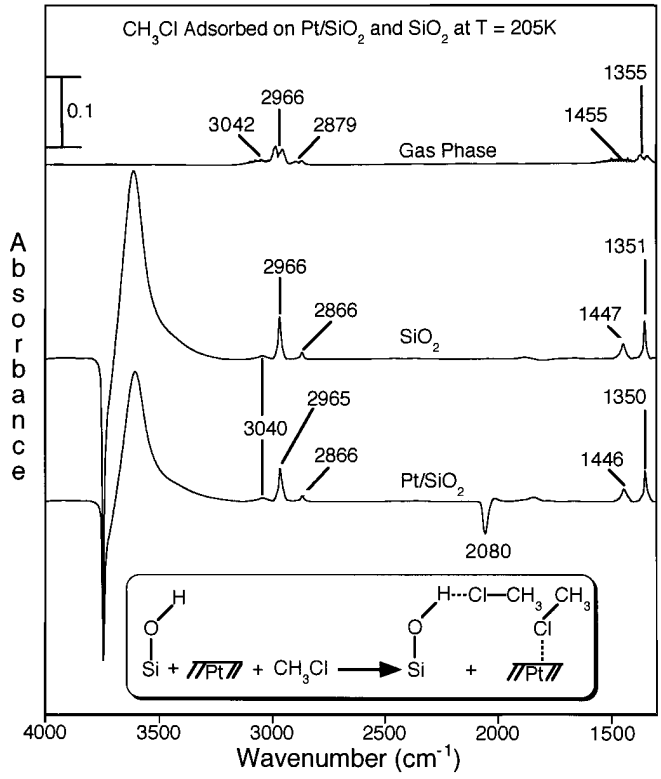

FIG. 1. FTIR spectra of CH_3Cl in the gas phase ($P = 7.1$ Torr) and adsorbed on SiO_2 and Pt/SiO_2 at $T = 205$ K at an equilibrium pressure of 7.1 Torr. For the adsorbed spectra, contributions from gas-phase CH_3Cl were subtracted out. The negative feature at 2080 cm^{-1} in the Pt/SiO_2 spectrum is due to displaced CO from the Pt surface.

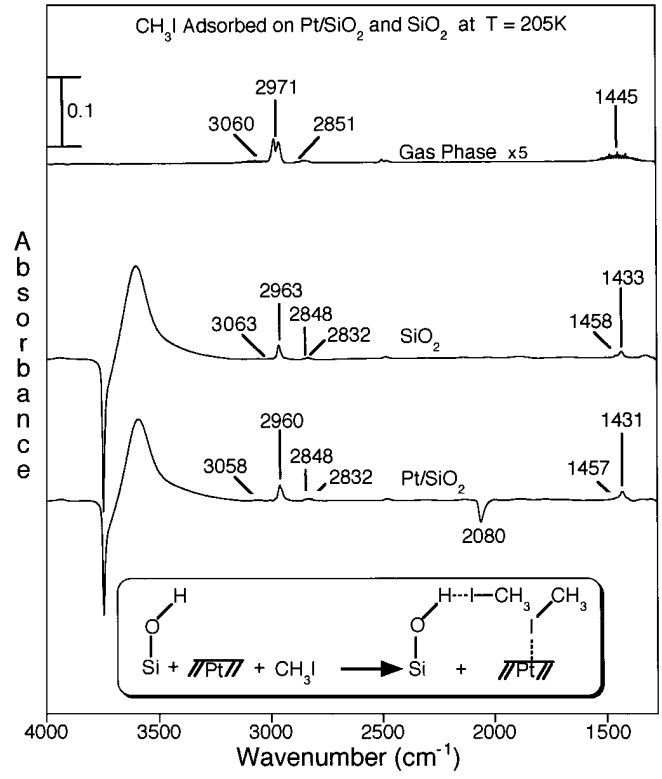

FIG. 2. FTIR spectra of CH_3I in the gas phase ($P = 2.0$ Torr) and adsorbed on SiO_2 and Pt/SiO_2 at $T = 205$ K at an equilibrium pressure of 2.0 Torr. For the adsorbed spectra, contributions from gas-phase CH_3I were subtracted out. The negative feature at 2080 cm^{-1} in the Pt/SiO_2 spectrum is due to displaced CO from the Pt surface.

bonding of the isolated hydroxyl groups with CH_3Cl (19, 20).

The spectra obtained for the pure SiO_2 samples are nearly identical to the Pt/SiO_2 samples, except that the bands in the Pt/SiO_2 spectra are slightly broader. There is also a negative feature in the Pt/SiO_2 spectrum near 2080 cm^{-1} which is due to displacement of some adsorbed CO from the Pt surface. The frequencies of the absorption bands for Pt/SiO_2 and SiO_2 are within one wavenumber of each other. This result can be somewhat expected considering the surface area of silica is significantly greater than for the Pt particles. We estimate the ratio of the surface area of silica to Pt to be 100 : 1 for these samples. The frequencies and assignments (21) of the absorption bands for gas phase CH_3Cl and CH_3Cl adsorbed on SiO_2, Pt/SiO_2 and Pt(111) (22), are given in Table 1.

The IR spectra of CH_3I in the gas phase and adsorbed on SiO_2 and Pt/SiO_2 at 205 K in the presence of an equilibrium pressure of gas-phase CH_3I are shown in Fig. 2 and display many of the same characteristics seen in the CH_3Cl spectra; i.e., CH_3I hydrogen bonds to surface hydroxyl groups. However, the CH_3I IR data are more complex compared to the CH_3Cl data. There appears to be more than one type of bonding interaction of CH_3I with the silica surface, which results in more than one band being assigned to some of the vibrational modes (see Table 1).

It has been shown by electron energy loss spectroscopy and X-ray photoelectron spectroscopy that alkyl halides bond to Pt(111) surfaces through the halogen atom (6, 7). Although we do not have direct evidence for the CH_3X–Pt interaction ($X = Cl$ and I), we will assume a similar type of bonding interaction for CH_3X adsorbed on silica-supported Pt. The proposed low-temperature bonding scheme for methyl halide adsorption on the Pt particles and the silica support are shown below the infrared spectra plotted in Figs. 1 and 2.

CH_3Cl and CH_3I Reactions on Pt/SiO_2 between 200 and 473 K

After introduction of 7.1 Torr of CH_3Cl to the IR sample cell, the cell was then evacuated. Upon evacuation of the gas phase, the temperature of the sample decreases by 5 degrees to 200 K. Infrared spectra recorded of the Pt/SiO_2 catalyst as a function of evacuation time is shown in Fig. 3. After evacuation of the IR cell for five minutes, the absorption bands for CH_3Cl adsorbed on the pure SiO_2 half

TABLE 1

Vibrational Assignment of Methyl Chloride and Methyl Iodide Adsorbed on Pt/SiO_2 and SiO_2 in the 1300–3200 cm^{-1} Spectral Region

Mode description (symmetry)[a]	CH_3Cl					CH_3I				
	Gas phase[a]	SiO_2[b]	Pt/SiO_2[b]	Pt(111)[c]	Pt/SiO_2[d]	Gas phase[a]	SiO_2[b]	Pt/SiO_2[b]	Pt(111)[e]	Pt/SiO_2[d]
C–H asym. stretch (e)	3042	3040	3040	n.o.[f]	n.o.	3060	3063	3058	3026–3029[g]	n.o.
C–H sym. stretch (a_1)	2966	2966	2965	2955	2950	2971	2963	2960	2909–2928	2943
Overtone (A_1)	2879	2866	2866	n.o.	n.o.	2851	2848, 2832[h]	2848, 2832	n.o.	n.o.
Asym. CH_3 deform. (e)	1455	1447	1446	1427	1429	1445	1458,1433	1457,1431	1410	1416
Sym. CH_3 deform. (a_1)	1355	1351	1350	1332	1337	1252	n.o.	n.o.	1216–1230	n.o.

[a] Ref. (21).
[b] In the presence of gas phase CH_3X.
[c] Ref. (22).
[d] CH_3X adsorbed on the surface of the Pt particles upon evacuation of gas phase CH_3X.
[e] Ref. (10)
[f] n.o. = not observed.
[g] Frequencies are coverge-dependent.
[h] Two species appear to be present.

of the sample disappear (see the bottom spectrum plotted in Fig. 3). However, there are two absorption bands in the C–H stretching region with frequencies of 2950 and 2967 cm^{-1} and two prominent bands in the CH_3 deformation region at 1429 and 1337 cm^{-1} present on the Pt/SiO_2 half of the sample. Upon evacuation for a longer period of time, three of the bands present in the Pt/SiO_2 spectrum at 2950, 1429, and 1337 cm^{-1} decrease in intensity.

Following evacuation of CH_3Cl for 60 min, the valve to the IR cell was closed to the pumps and the sample was then

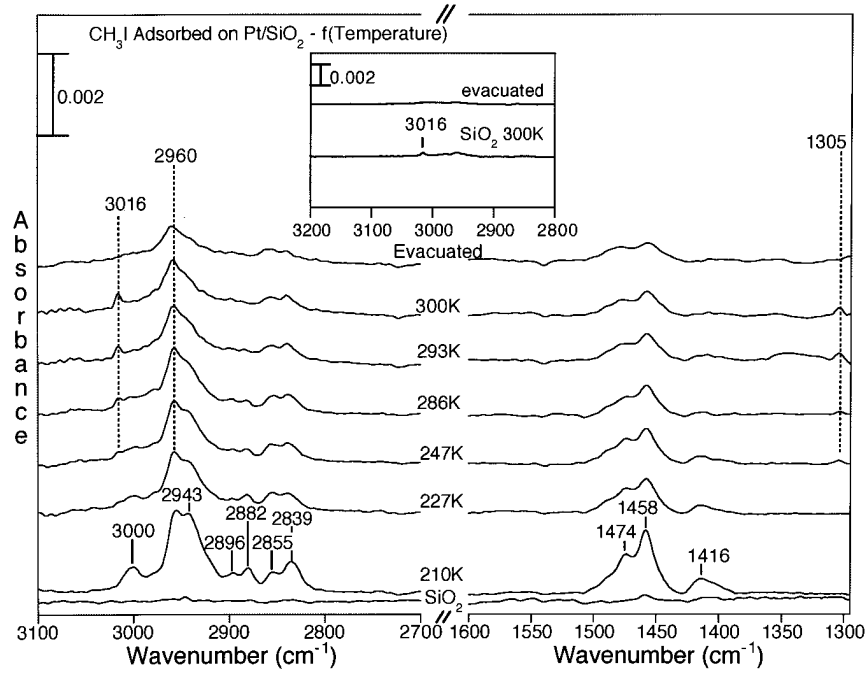

FIG. 3. Infrared spectra recorded of a Pt/SiO_2 catalyst as a function of evacuation time after initially introducing 7.1 Torr of gas-phase CH_3Cl. The absorption bands in the spectra are due to CH_3Cl and CH_3 adsorbed on the Pt particles. Also shown is the spectrum recorded for the pure SiO_2 sample. After evacuation for 5 min at 200 K, no infrared absorption bands are present on samples containing only SiO_2.

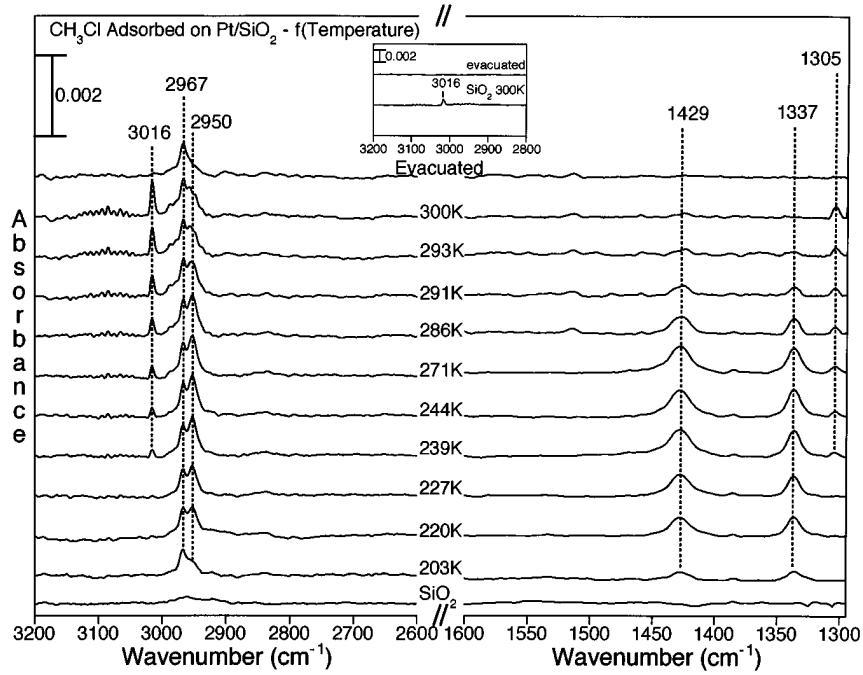

FIG. 4. Infrared spectra recorded of a Pt/SiO_2 catalyst as a function of temperature from 203 to 300 K after adsorption and 60 min of evacuation of CH_3Cl. The bottom spectrum shows there is no adsorbed species on pure SiO_2 at 203 K. The IR cell valve was closed off from the pumps so that gas-phase species could be detected. As the sample is warmed above 227 K, two absorption bands become apparent at 3016 and 1305 cm^{-1}. The 3016 cm^{-1} band clearly shows rotational structure which is characteristic of gas-phase species. These two bands are associated with gas-phase methane. The inset is that for pure SiO_2 after heating to 300 K with the sample valve closed and after evacuation. Only the 3016 cm^{-1} band for gas-phase CH_4 is seen in the spectral region extending from 2800 to 3200 cm^{-1}. Again, no other bands due to adsorbed hydrocarbon species are seen in the pure SiO_2 spectrum.

warmed (see Fig. 4). Initially, the bands at 2950, 1429, and 1337 cm^{-1} increase in intensity as the sample is heated but then decrease as gas-phase methane is formed (methane absorptions at 3016 and 1305 cm^{-1}) (23). Although it is unclear why the bands at 2950, 1429, and 1337 cm^{-1} initially increase in intensity upon warming, it is clear that upon heating to 300 K these bands are no longer present in the spectrum. Besides the formation of gas-phase CH_4 and the disappearance of adsorbed CH_3Cl, the band at 2967 cm^{-1} increases upon warming from 200 to 300 K and remains a lone band in the spectrum recorded at room temperature upon evacuation. The inset in Fig. 4 shows the spectrum from 2800 to 3200 cm^{-1} for the pure SiO_2 side of the sample after warming to 300 K. Only an absorption band due to gas-phase methane at 3016 cm^{-1} is apparent in the spectrum.

The three bands at 2950, 1429, and 1337 cm^{-1} correlate with methyl chloride adsorbed on the Pt surface. The 2950 cm^{-1} band is assigned to the symmetric C–H stretch and the two bands at 1429 and 1337 cm^{-1} are assigned to the symmetric and asymmetric methyl deformation modes (see Table 1). The frequencies of the vibrational modes of CH_3Cl adsorbed on Pt particles in Pt/SiO_2 are in remarkably good agreement to the frequencies observed for CH_3Cl adsorbed on Pt(111) (22).

As noted above, after evacuation of methane from the IR cell at 300 K, the IR spectrum of Pt/SiO_2 is characterized by the one band at 2967 cm^{-1}. Upon further warming to higher temperatures, the band at 2967 cm^{-1} decreases in intensity and the production of gas-phase methane is again apparent in the infrared spectrum. As shown in Fig. 5, the 3016 cm^{-1} band becomes quite evident at $T = 373$ K and increases in intensity as the sample is warmed to 473 K and then kept at that temperature for 30 min.

The conversion of methyl chloride to methane most likely proceeds through adsorbed methyl groups on the surface (Eq. [2]). The band at 2967 cm^{-1} may be attributed to adsorbed methyl groups formed from the dissociation of CH_3Cl. Adsorbed methyl groups can react with hydrogen atoms to form methane (Eq. [3]),

$$CH_3Cl \rightarrow CH_3(a) + Cl(a) \qquad [2]$$

$$CH_3(a) + H(a) \rightarrow CH_4(g). \qquad [3]$$

The available hydrogen can come from several sources. One possible source is from dehydrogenation of CH_3 groups to form CH_2, CH, or C. Other sources of hydrogen are from background hydrogen in the infrared cell or residual hydrogen left on the catalyst after reduction. The reaction of CH_3 to form CH_4 is limited by the amount of available hydrogen. In experiments where H_2 was added to the IR cell at 300 K, all of the CH_3 groups immediately react to form CH_4, as evidenced by the disappearance of the 2967 cm^{-1} band upon hydrogen addition.

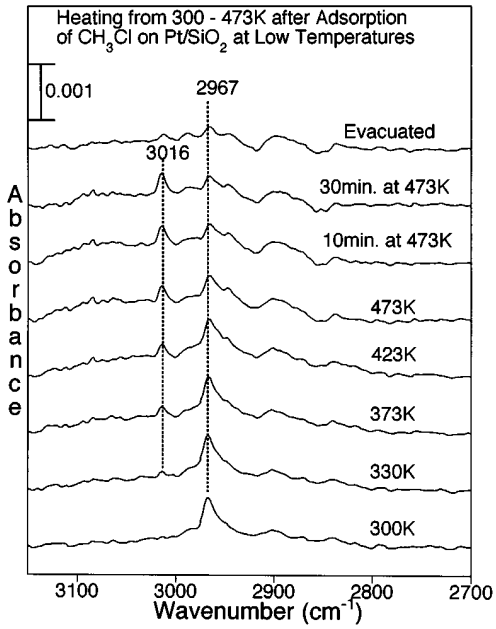

FIG. 5. Infrared spectra recorded of a Pt/SiO_2 catalyst in the C–H stretching region as a function of temperature from 300 to 473 K after adsorption of CH_3Cl at low temperatures. The spectrum recorded at 300 K is the same as the top spectrum labeled "evacuated" in Fig. 4. After evacuation, the IR cell valve was again closed off from the pumps so that gas-phase species could be detected. Gas-phase methane is observed in the spectrum as the sample is warmed. After heating to 473 K, the sample was kept at that temperature for 30 min prior to evacuation.

Similar reactions to CH_3Cl are observed for CH_3I after introduction of 2 Torr of gas into the IR cell at 210 K. The infrared spectrum recorded of the Pt/SiO_2 catalyst after evacuation of CH_3I for 75 min at 210 K is shown in Fig. 6. There are more bands apparent in the CH_3I–Pt/SiO_2 spectrum than for the CH_3Cl–Pt/SiO_2 spectrum. There are no absorption bands due to adsorbed species on the silica half of the sample after evacuation for 75 min at 210 K. The bands at 3000, 2896, 2882, 2855, 2839, 1474, and 1458 cm^{-1} in the spectrum shown in Fig. 6 are identical to bands found in the spectrum of adsorbed CH_3I on SiO_2 after five minutes of evacuation (not shown). The bands at 2943 and 1416 cm^{-1} were not found in the SiO_2 spectrum and are, therefore, assigned to CH_3I adsorbed on the Pt particles (see Table 1). Although not fully understood, the bands due to CH_3I adsorbed on SiO_2 are absorbed on Pt/SiO_2 but not SiO_2 after 75 minutes of evacuation.

As the sample is warmed to room temperature with the IR cell valve closed, the bands at 3016 and 1305 cm^{-1} for gas-phase methane grow in. After evacuation of the sample cell at 300 K, there remains a lone band in the spectrum with a frequency of 2960 cm^{-1}. The band at 2960 cm^{-1} is eventually lost after heating further to 473 K, concurrent with the production of methane (spectra not shown). The results for CH_3I are very similar to those shown for CH_3Cl and it appears that similar processes are occurring, i.e., dissociative adsorption of the parent methyl halide to produce methyl groups on the surface which are converted to CH_4 between 200 and 473 K.

Reaction of CH_3Cl and CH_3I with Hydrogen on Pt/SiO_2 and SiO_2 at 473 K

Reaction of gaseous CH_3Cl and CH_3I in the presence of Pt/SiO_2 was followed with and without the addition of H_2 to the IR cell. Figure 7 (left panel) shows the infrared spectrum recorded of the gas phase in the 2600–3400 cm^{-1} spectral range immediately after the introduction of 10.0 Torr of methyl chloride and no hydrogen at 300 K. As can be seen by the band at 3016 cm^{-1} in the spectrum, the conversion of methyl chloride to methane has already begun. After recording the initial spectrum, the catalyst temperature was raised to 473 K at a heating rate of approximately 7 K/s. After 30 min, the loss of methyl chloride had leveled off. The IR spectrum recorded after 30 min of reaction clearly shows production of methane. Concomitant with the growth of bands associated with CH_4 is the loss of about 20% of the methyl chloride. These features can be more easily seen in the difference spectrum shown in Fig. 7.

The reaction of CH_3Cl on Pt/SiO_2 was also monitored in the presence of hydrogen. Figure 7 (right panel) shows the spectrum of approximately 7 Torr each of CH_3Cl and H_2 immediately after introduction into the IR cell at room temperature in the presence of the Pt/SiO_2 catalyst. Again the 3016 cm^{-1} band in the spectrum indicates methane formation at room temperature. Immediately after warming the catalyst to 473 K, all of the methyl chloride converts to methane and HCl, as indicated by an envelope of bands centered around 2800 cm^{-1} (see inset in Fig. 7). No other reaction products, e.g, C_2H_6 or CH_2Cl_2 are observed.

The same experiments were done in the presence of SiO_2 alone without Pt. Although in the difference spectrum for SiO_2 shown at the bottom of Fig. 7 there appears to be some loss of CH_3Cl, there is no formation of gas-phase methane or HCl when Pt is not present (24). There are no surface bound species left on the silica surface after reaction of CH_3Cl with SiO_2 at these temperatures.

Similar reaction with methyl iodide show that methyl iodide over Pt/SiO_2 dissociates to a much lesser extent than methyl chloride over a Pt/SiO_2 catalyst. For methyl chloride the reaction leveled off after 3 min, methyl iodide shows a very slow, steady loss of about 3% total over a period of 30 min in the absence of hydrogen (Fig. 8, left panel). Even in the presence of hydrogen, the conversion of methyl iodide to methane was limited (7% loss of methyl iodide after 30 min—right panel, Fig. 8) compared to CH_3Cl reaction. HI was not detected in either experiment as no bands near 2230 cm^{-1}, with a spacing on the order of 6 cm^{-1}, were apparent in the IR spectrum. Taking these results together, i.e., lack of HI formation and the limited amount of CH_3I decomposition, suggests that an iodine overlayer

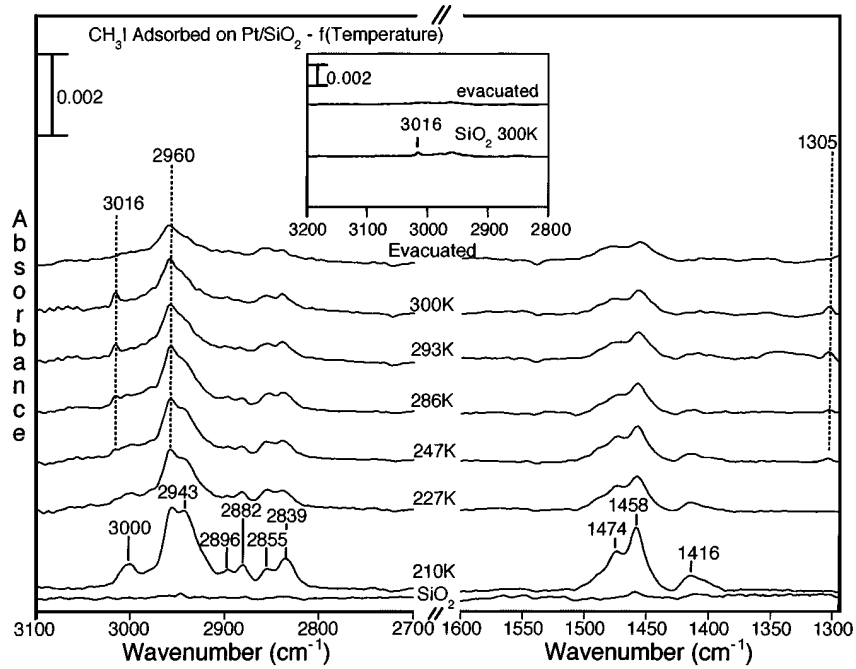

FIG. 6. Infrared spectra recorded of a Pt/SiO_2 catalyst as a function of temperature from 210 to 300 K after introducing 2 Torr of CH_3I and subsequent evacuation of CH_3I for 75 min. The IR cell valve was closed off from the pumps so that gas-phase species could be detected. Gas-phase methane is detected at temperatures of 247 K and above. The bottom spectrum is that of SiO_2 after evacuation for 75 min, showing no adsorption of CH_3I. The inset shows the spectrum of SiO_2 after warming to 300 K. The absorption band due to gas-phase CH_4 is seen.

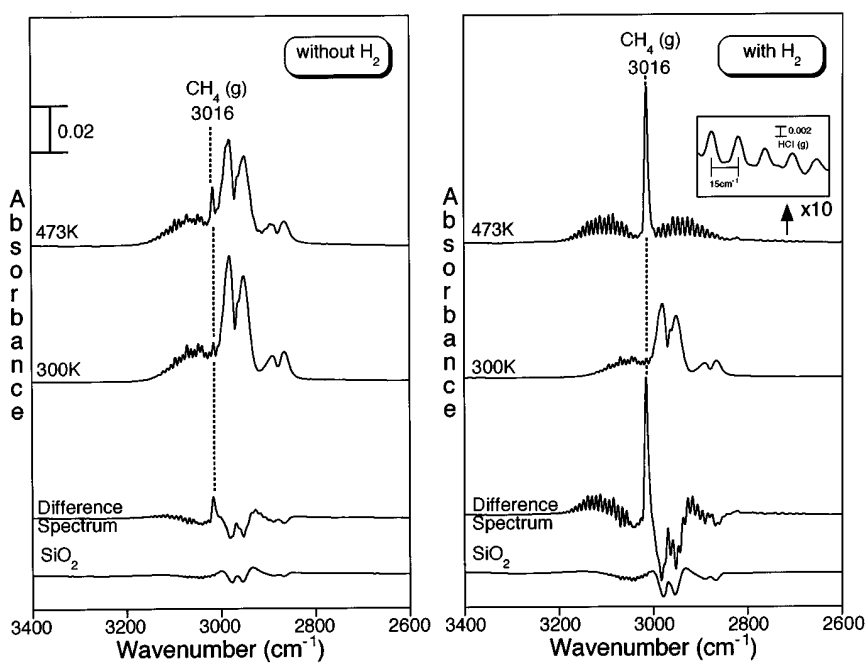

FIG. 7. Infrared spectra of gas-phase CH_3Cl in the presence of a Pt/SiO_2 catalyst without hydrogen (left) and with hydrogen (right). *Left:* Room temperature infrared spectrum of gas-phase CH_3Cl in the presence of Pt/SiO_2 and after reaction at $T = 473$ K. Difference spectrum showing the loss of some of the intensity of the CH_3Cl bands and the growth of product bands as the reaction proceeds. A difference spectrum is also shown for reaction of CH_3Cl on SiO_2 (bottom spectrum). No methane is formed in the absence of Pt. *Right:* Room temperature infrared spectrum of CH_3Cl and H_2 in the presence of Pt/SiO_2 and the infrared spectrum recorded of the gas phase after heating the Pt catalyst to $T = 473$ K. The difference spectrum shows there is complete conversion of methyl chloride to methane and hydrogen chloride. A difference spectrum recorded for reaction in the presence of SiO_2 shows no formation of methane or hydrogen chloride. The inset shows an expanded view of part of the spectrum where HCl bands are observed.

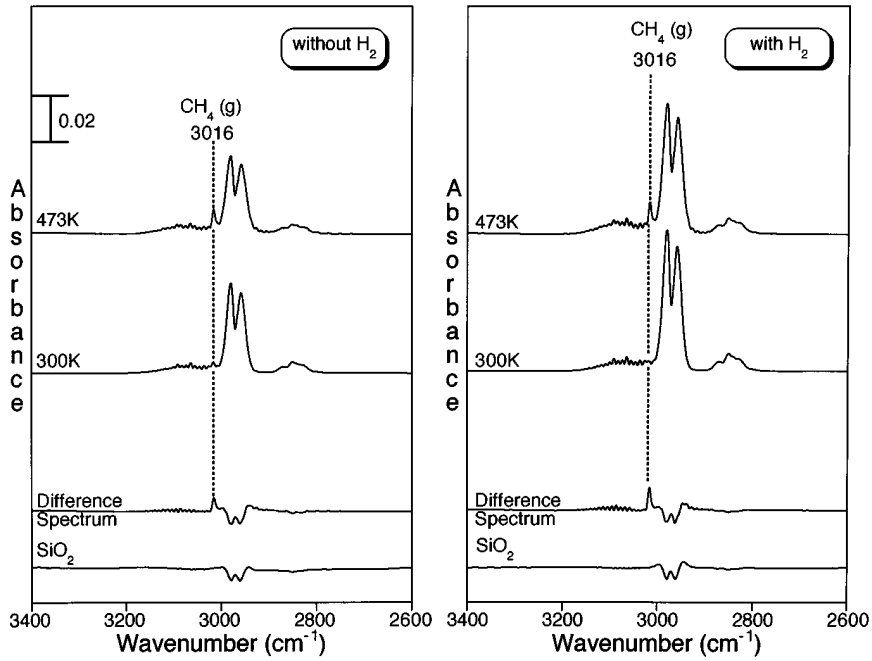

FIG. 8. Infrared spectra of gas-phase CH_3I in the presence of a Pt/SiO_2 catalyst without hydrogen (left) and with hydrogen (right). *Left:* Room temperature infrared spectrum of gas-phase CH_3I in the presence of Pt/SiO_2 and after reaction at $T = 473$ K. Difference spectrum showing the loss of some of the intensity of the CH_3I bands and the growth of product bands as the reaction proceeds. A difference spectrum is also shown for reaction of CH_3I on SiO_2. No methane is formed in the absence of Pt particles. *Right:* Room temperature infrared spectrum of CH_3I and H_2 in the presence of Pt/SiO_2 and the infrared spectrum recorded of the gas phase after heating the Pt catalyst to $T = 473$ K for 30 min. The difference spectrum shows there is complete conversion of methyl chloride to methane and hydrogen chloride. A difference spectrum recorded shows only partial conversion of methyl iodide to methane and no evidence of hydrogen iodide.

is poisoning the surface. Experiments with CO corroborate this suggestion, as there is a 95% decrease in the amount of CO that can adsorb on the Pt surface after the CH_3I reaction. The decrease in CO chemisorption capacity indicates that sites are indeed being blocked.

Similar reactions were done for a pure silica sample. There appears to be some loss of gas-phase methyl iodide after reaction with silica, although, there was no production of methane after reaction of methyl iodide in the presence or absence of hydrogen. However, SiO_2 does react with CH_3I at 473 K to some extent to form surface-bound products. A spectrum recorded of the silica surface after reaction of CH_3I shows evidence for a surface bound species identified as $SiOCH_3$ groups.

Photo-Assisted Decomposition of CH_3Cl on Pt/SiO_2

It is well known that alkyl halides adsorbed on metal surfaces can photodissociate with photons of lower energy than in the gas phase because of substrate mediated mechanisms in metal surface photochemistry (2, 4, 8, 9, 25, 26). In many cases, wavelengths effective toward bond dissociation for adsorbed molecules are in the solar spectrum which begins near 300 nm (3.8 eV). The lower energy threshold suggests that metals can be used as effective photo-assisted catalysts in the presence of solar light.

Thus far, most studies on metal surface photochemistry have been done on single crystal surfaces in ultrahigh vacuum (UHV). The pristine environment of an ultrahigh vacuum chamber is ideal for determining fundamental aspects of surface photochemistry, but not so for practical use. The use of solar radiation as a method for the decomposition of chlorinated organics adsorbed on semiconductors has been studied in detail (27). Here, we explore the use of solar radiation as a means for decomposing CH_3Cl on Pt/SiO_2.

Irradiation experiments were done using a broadband Hg Arc lamp with a H_2O filter in place to remove infrared radiation. Several experiments were done using different UV/VIS cutoff filters and different substrate temperatures in order to determine the wavelength dependence and if thermal and photochemical effects could be distinguished.

The UV/VIS spectrum of Pt/SiO_2 is shown in Fig. 9. The Pt/SiO_2 catalyst was placed at normal incidence with respect to the incident light. The spectrum is plotted as extinction versus wavelength as opposed to absorbance versus wavelength because the sample does scatter light. (Extinction refers to the loss of light due to absorption and scattering (28).) A peak near 270 nm is seen in the Pt/SiO_2 spectra whereas no such peak is seen for pure SiO_2 (not shown). The spectrum clearly shows that Pt particles absorb light between 200 and 500 nm. In contrast, CH_3Cl does not absorb light at these wavelengths (29).

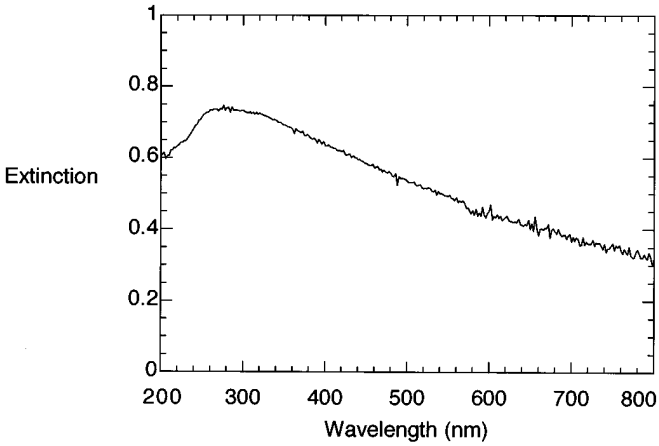

FIG. 9. UV/VIS spectrum of a Pt/SiO_2 catalyst plotted as extinction vs wavelength. The sample was at normal incidence with respect to the light source.

Figure 10 shows the infrared spectrum of Pt/SiO_2 before and after photolysis of adsorbed CH_3Cl with the full Hg arc lamp (top spectrum). The IR spectra before and after irradiation using broadband cutoff filters are also shown. The wavelengths noted in Fig. 10 are the wavelengths for 0% transmittance for each of the filters. In these experiments, the sample was prepared by introducing approximately 7 Torr of CH_3Cl into the sample cell at 180 K followed by evacuation for 2 min. After 2 min, the sample valve was closed to the pumping system. With the full Hg arc lamp ($\lambda > 230$ nm), the results show that CH_4 is formed upon irradiation and that CH_3Cl is lost. There is also an increase in the amount of methyl groups adsorbed on the surface as indicated by a growth in the band at 2967 cm^{-1} after irradiation. The spectra in Fig. 10 show that some methane is formed at all wavelengths, but with less efficiency than at the shorter wavelengths. The amount of methane and adsorbed methyl groups formed from irradiation with 460 and 500 nm light is nearly the same as that formed without irradiation. These results show that there is some wavelength dependence for the CH_3Cl–Pt/SiO_2 photoreaction and that methane and adsorbed methyl are formed with greater propensity using photons at wavelengths below 380 nm.

In order to distinguish between photochemical and thermal effects, the effect of substrate temperature on the photo-assisted decomposition of CH_3Cl was examined. Figure 11 shows the infrared spectra recorded after photolysis with the full Hg arc lamp of CH_3Cl adsorbed on Pt/SiO_2 at two different temperatures: 148 and 208 K. The data show that there is less methane formed, approximately 50% less, when the substrate is held at 148 K compared to the substrate held at 208 K. In addition, there is a similar increase in the amount of methyl formed at the two temperatures. These results show there is a significant temperature dependence for the photoreaction.

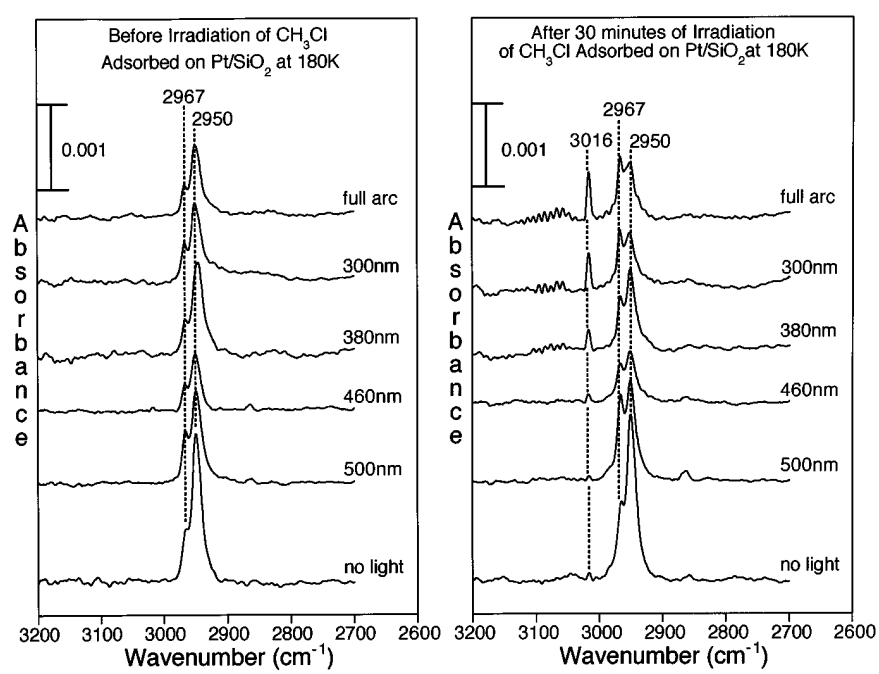

FIG. 10. *Left:* Infrared spectra recorded of CH_3Cl adsorbed on Pt/SiO_2 before broadband irradiation. *Right:* Infrared spectra recorded after 30 min of irradiation with the full Hg arc lamp and after irradiation with broadband cutoff filters. The wavelengths noted above are for the 0% transmittance wavelength for each filter.

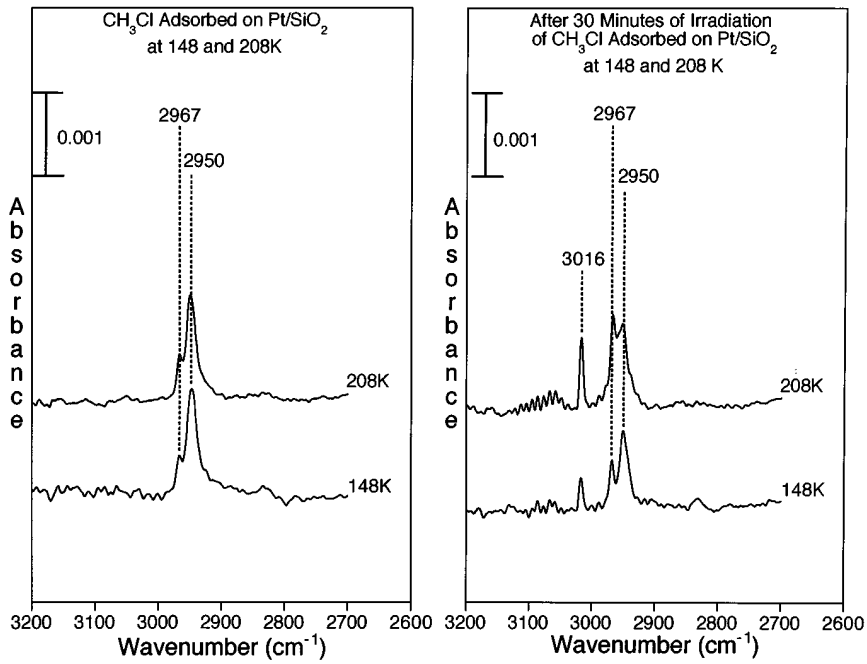

FIG. 11. *Left:* Infrared spectra recorded of CH_3Cl adsorbed on Pt/SiO_2 at 148 and 208 K before broadband irradiation. *Right:* Infrared spectra recorded after broadband irradiation with the full Hg arc for 30 min at the two different temperatures. Less methane is produced when the sample was irradiated at a sample temperature of 148 K compared to 208 K.

DISCUSSION

Bonding of CH_3Cl and CH_3I to Pt/SiO_2

The infrared spectra can be used to determine the nature of the bonding of CH_3Cl on SiO_2 and Pt/SiO_2. It is clear from the IR data that hydroxyl groups on the silica surface participate in the bonding of CH_3Cl. In general, halogenated hydrocarbons hydrogen bond to silica hydroxyl groups (19). The hydrogen bonding interaction is most likely between the halogen atom and the surface OH group. The spectra obtained for Pt/SiO_2 and SiO_2 are nearly identical, except for small frequency displacement of some of the bands and, as noted, a slight increase in the breadth of the bands.

Upon evacuation of gas-phase methyl chloride, all of the hydrogen-bonded CH_3Cl desorbs from the silica surface. Some CH_3Cl remains bonded to the Pt particles upon evacuation. The assignment of the bands associated with CH_3Cl adsorbed on Pt/SiO_2 and Pt(111) surface are given in Table 1. The frequencies of these bands are within 5 cm^{-1} of the bands observed for CH_3Cl adsorbed on Pt(111) (22). Both the symmetric and asymmetric methyl deformation modes are present in the spectrum of CH_3Cl adsorbed on the Pt particles. Although the particle size of 2 nm is near the theoretical limit for application of the metal surface selection rule (30), a consideration of the metal surface selection rule would imply that the C_{3v} axis in adsorbed CH_3Cl is tilted with respect to the surface plane.

Because there appears to be more than one type of bonding site or bonding interaction, CH_3I adsorption on SiO_2 and Pt/SiO_2 is more complicated than CH_3Cl adsorption. As noted in the Results section, there are some similarities; for example, hydroxyl groups do participate in bonding of CH_3I on silica.

Vibrational Assignment of Adsorbed Methyl Groups

Besides adsorbed CH_3Cl and CH_3I, there is an adsorbed hydrocarbon fragment present after adsorption of CH_3Cl and CH_3I at low temperatures. The spectrum for this species is characterized by a single IR absorption band near 2965 cm^{-1}. A possible assignment for this band is that it is the C–H stretching motion in adsorbed methyl groups. Table 2 lists the vibrational frequencies obtained from electron energy loss and reflectance absorption infrared spectroscopy for methyl groups adsorbed on Pt(111). Also given in Table 2 are the vibrational frequencies of $(Ph_3P)_2Pt(CH_3)_2$ (31).

If the band near 2965 cm^{-1} (2967-CH_3Cl and 2960-CH_3I) was assigned to the symmetric C–H stretching motion in adsorbed CH_3, this would indicate a shift to higher frequency by approximately 84 cm^{-1} for this band from that of CH_3 adsorbed on Pt(111). Only the symmetric stretch and an overtone of the same symmetry are apparent in the infrared spectrum of methyl groups adsorbed on Pt(111). Applying the metal surface selection rule, the IR data indicate that methyl groups are bonded to Pt(111) with their C_{3v} axes perpendicular to the surface (10). The assignment of the

TABLE 2

Vibrational Assignment of Coordinated and Adsorbed CH_3 Groups

Mode description (symmetry)	CH_3–Pt(111)[a, b]			CH_3–Pt/SiO_2[d]	
	IR (CH_3I)[a]	EELS (CH_3I)[b]	$(Ph_3P)_2Pt(CH_3)_2$[c]	(CH_3Cl)	(CH_3I)
C–H asym. stretch (*e*)	n.o.[e]	2925	2934	n.o.	n.o.
C–H sym. stretch (a_1)	2879	2925	2878	2967	2960
Overtone (A_1)	2756	2775	2806	n.o.	n.o.
CH_3 asym. deform. (*e*)	n.o.	1425	n.r.[f]	n.o.	n.o.
CH_3 sym. deform. (a_1)	n.o.	1165	n.r.	n.o.	n.o.

[a] Ref. (10).
[b] Ref. (6).
[c] Ref. (31).
[d] This work.
[e] n.o. = not observed.
[f] n.r. = not reported.

lone band near 2965 cm^{-1} in the Pt/SiO_2 spectrum to the symmetric stretch would also indicate that the molecule has C_{3v} symmetry on Pt/SiO_2. Alternatively, if the band was due to the asymmetric C–H stretching motion it would indicate that the molecular axis for CH_3 would be parallel to the surface. As it is very difficult to assign the spectrum of hydrocarbon moiety based on a lone band in the spectrum, we assign the lone band at 2965 cm^{-1} using the assignment of Fan and Trenary, i.e., to the symmetric C–H stretch of adsorbed methyl (10). Although it should be noted that another possible assignment of the band near 2965 cm^{-1} is that of a more dehydrogenated species such as a methylene group. Zaera has presented evidence for methylene groups adsorbed on Pt(111) from the decomposition of methyl groups near room temperature (5, 32).

Reaction of CH_3Cl and CH_3I on Pt/SiO_2

Reactions [4]–[6] summarize the chemistry of CH_3Cl and CH_3I adsorbed on Pt/SiO_2 in the 200–473 K temperature range as determined from the infrared data presented here:

$$CH_3X(a) \xrightarrow{200-300\ K} CH_3(a) + X(a) \quad (X = Cl, I) \quad [4]$$

$$CH_3(a) + H(a) \xrightarrow{200-473\ K} CH_4(g) \quad [5]$$

$$H(a) + Cl(a) \xrightarrow{473\ K} HCl(g) \quad [6a]$$

$$H(a) + I(a) \xrightarrow{473\ K} \not{\rightarrow} HI(g) \quad [6b]$$

Initially, the carbon–halogen bond is dissociated in adsorbed methyl halide (Eq. [4]). The adsorbed methyl fragment produced in the dissociation step goes on to react with adsorbed hydrogen to form methane in the temperature range extending from approximately 230 to 473 K (Eq. [5]). As discussed previously, this large temperature range is related to the availability of hydrogen on the surface. The reactions shown in Eq. [6], i.e., removal of the strongly bonded halogen atom, is an important consideration if the catalyst is to maintain active.

In these experiments, HCl is produced during CH_3Cl and H_2 reaction over Pt/SiO_2 but HI, from reaction of CH_3I, does not form. This result indicates that the decreased activity of Pt/SiO_2 toward methyl iodide decomposition is due to the formation of a stable iodine adlayer that can not be easily removed. The deposited iodine layer poisons the Pt surface and decreases its activity. Therefore, the data suggest that the rate limiting step in the decomposition of methyl halides is not the initial step of the reaction involving carbon–halogen bond dissociation (Eq. [4]) but the last step involving halogen desorption (Eq. [6]). The differences in the reactions of CH_3Cl and CH_3I and the removal of the halogen atom in these reactions is related to the reaction energetics as discussed in detail in the next section.

The results presented here for CH_3Cl decomposition at 473 K are in agreement with several studies reported in the literature. In a study by Fung and Sinfelt, the kinetics of the catalytic decomposition of methyl chloride with hydrogen to give methane and hydrogen chloride were measured for a variety of metals supported on silica in order to establish activity patterns for several hydrogenolysis reactions (33). The most active metal for methyl chloride hydrogenoly-

sis was Pt which had a catalytic activity approximately 2–4 times greater than Ir and nearly 5–10 times greater than Rh and Pd. In another study of methyl chloride and hydrogen reaction on Pt thin films, methane was the only hydrocarbon product formed (34).

Recently, the adsorption and chemistry of CH_3Cl and CH_3I on Pd/SiO_2 were studied with IR and mass spectroscopy (35). Gaseous CH_4 and HCl during CH_3Cl decomposition were detected with mass spectrometry at temperatures as low as 213 K. The IR data supported the presence of CH_3 groups from CH_3Cl and CH_3I decomposition on Pd/SiO_2 on the surface at low temperatures. The results obtained here on Pt/SiO_2 catalysts are qualitatively similar to the results obtained for reaction of CH_3Cl and CH_3I on Pd/SiO_2 catalysts.

Reaction Energetics

The activation energy of desorption, assuming a frequency factor of 10^{13} s^{-1}, is estimated to be 48 and 53 kcal/mol for Cl and I, respectively (36, 37) from ultrahigh vacuum studies on Pt(111) surfaces. These are large barriers for desorption of the halogen and are too high to overcome to any appreciable extent at 473 K, so it is not expected that the halogen atoms will thermally desorb from the Pt catalyst during reaction.

Energy diagrams for the reaction $CH_3X + H_2 \rightarrow CH_4 + HX$. (where $X = Cl$ and I) are presented in the left panel of Fig. 12. The bond dissociation energies, heats of adsorption and heats of formation used to construct Fig. 12 are given in Table 3. For the $CH_3Cl + H_2$ reaction, the overall exothermicity is 27 kcal/mol. The apparent activation energy for this reaction has been determined by Fung and Sinfelt to be 15 kcal/mol (33). The energy levels for the $CH_3I + H_2$ reaction are shown. This reaction is exothermic by 29 kcal/mol. However, it can be seen from the energy diagram that there is a large energy barrier for formation of CH_4 and HI from CH_3, I, and H of at least 32 kcal/mol. In general because of the weaker C–I bond in alkyl iodides compared to the C–Cl bond in alkyl chlorides, the activation barrier is lower for C–I bond dissociation. However, based on the reaction products that are formed, the extent of product formation and the energy diagram shown in Fig. 12, it is clear that the energy barrier for formation of HI and CH_4 is too high to occur to any great extent under the pressure and temperature conditions of this study. Instead, the reaction for CH_3I appears to be stoichiometric as shown in the energy diagram in the right panel of Fig. 12. The fact that the amount of CO that can be adsorbed on the catalyst after reaction of CH_3I is only 5% of its original amount is consistent with this interpretation.

Photo-Assisted Decomposition Reactions–CH_3Cl Adsorbed on Pt/SiO_2

The data clearly show that methane is formed upon irradiation of CH_3Cl adsorbed on Pt/SiO_2. There is a wavelength dependence; i.e., light of wavelengths below 380 nm are more effective in forming methane. Since CH_3Cl does not absorb light at this wavelength and the Pt/SiO_2 substrate does, the results are consistent with a substrate mediated process. The photo-assisted reaction appears to have a definite thermal component because there is a temperature dependence as shown from the decrease in the amount of methane formed at 148 compared to 208 K. The wavelength dependence may arise from the fact that the Pt particles can absorb light at the shorter wavelengths to a greater extent as shown by the UV/VIS spectrum (Fig. 9). Light energy can be then converted to thermal energy. It is difficult to distinguish between thermal and photolysis reactions because the same products are being formed in both cases. There may in fact be a combination photothermal effect that is operative for the photo-assisted decomposition of CH_3Cl adsorbed on Pt/SiO_2.

TABLE 3

Bond Dissociation Energies, Heats of Adsorption, and Heats of Formation

Energy	kcal/mol
Bond dissociation energies	
$D_0(Cl–CH_3)$	85[a]
$D_0(H–Cl)$	103[a]
$D_0(I–CH_3)$	57[a]
$D_0(H–I)$	71[a]
$D_0(Pt–H)$	62[b]
$D_0(Pt–CH_3)$	32[b]
$D_0(H–H)$	104[a]
$D_0(H–CH_3)$	105[a]
Heats of adsorption[c]	
$H_{ads}(CH_3Cl)$	−8[d]
$H_{ads}(CH_3I)$	−15[d]
$H_{ads}(Pt–Cl)$	48[e]
$H_{ads}(Pt–I)$	53[f]
Heats of formation	
$H_f^\circ(CH_3Cl)$	−19[a]
$H_f^\circ(HCl)$	−22[a]
$H_f^\circ(CH_3I)$	−4[a]
$H_f^\circ(HI)$	6[a]
$H_f^\circ(CH_4)$	−18[a]

[a] Ref. (38).
[b] Ref. (39).
[c] Heats of Adsorption calculated from TPD data, assuming a nonactivated desorption process.
[d] Ref. (6).
[e] Ref. (36).
[f] Ref. (37).

ACKNOWLEDGMENTS

Acknowledgment is made to the donors of the Petroleum Research Fund, administered by the American Chemical Society, for partial support of this research. The authors also gratefully acknowledge the National

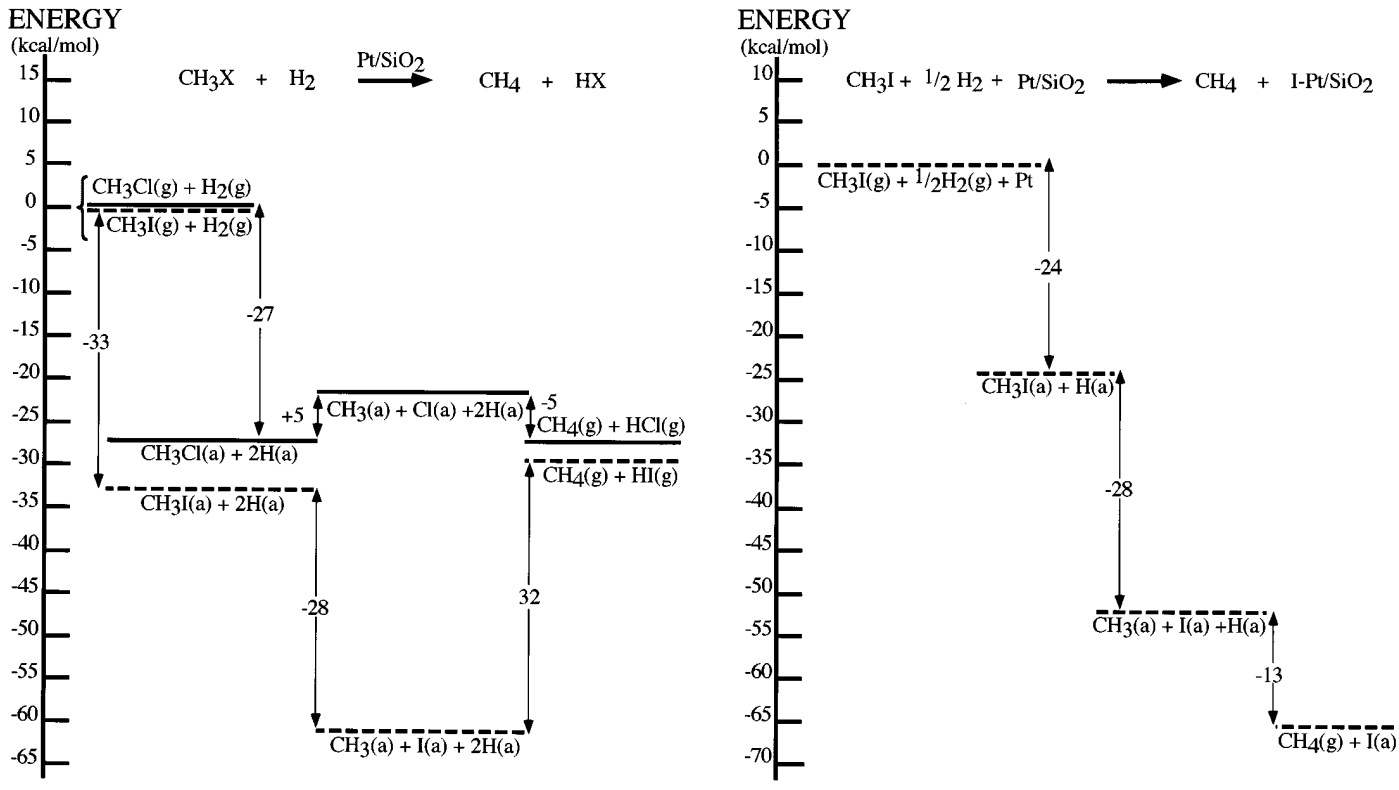

FIG. 12. *Left:* Reaction energetics for the reaction $CH_3X + H_2 \rightarrow CH_4 + HX$ (where $X =$ Cl and I). *Right:* Reaction energetics for the reaction $CH_3I + Pt \rightarrow CH_4 + Pt–I$. See text for further details.

Science Foundation (Grant CHE- 9300808) for support of this research. The authors would like to thank Dr. Mauro Briceno and Leonardo Martinez for the TEM measurements.

REFERENCES

1. Zaera, F., *Acc. Chem. Res.* **25**, 260 (1992).
2. (a) Zhou, X.-L., Zhu, X.-Y., and White, J. M., *Acc. Chem. Res.* **23**, 327 (1990); (b) *Surf. Sci. Rep.* **13**, 73 (1991) and references therein.
3. Lin, J.-L., and Bent, B. E., *J. Vac. Sci. Technol. A* **10**, 2202 (1992).
4. Roop, B., Lloyd, K. G., Costello, S. A., Campion, A., and White, J. M., *J. Chem. Phys.* **91**, 5103 (1989).
5. Zaera, F., and Hoffman, H., *J. Phys. Chem.* **95**, 6297 (1991).
6. Henderson, M. A., Mitchell, G. E., and White, J. M., *Surf. Sci.* **184**, L325 (1987).
7. Liu, Z.-M., Akhter, S., Roop, B., and White, J. M., *J. Am. Chem. Soc.* **110**, 8708 (1988).
8. Solymosi, F., and Revesz, K., *J. Am. Chem. Soc.* **113**, 9145 (1991).
9. Zhou, Y., Feng, W. M., Henderson, M. A., Roop, B., and White, J. M., *J. Am. Chem. Soc.* **110**, 4447 (1988).
10. Fan, J., and Trenary, M., *Langmuir,* **10**, 3649 (1994).
11. Somorjai, G. A., "Introduction to Surface Chemistry and Catalysis." Wiley, New York, 1994.
12. Windawi, H., and Wyatt, M., *Platinum Met. Rev.* **37**, 186 (1993).
13. McGee, K. C., Capitano, A. T., and Grassian, V. H., *Langmuir,* **10**, 632 (1994).
14. Driessen, M. D., and Grassian, V. H., *J. Phys. Chem.,* **99**, 16519 (1995).
15. Beebe, T. P., Jr., Gelin, P., and Yates, J. T., Jr., *Surf. Sci.* **148**, 526 (1984).
16. Ballinger, T. H., Wong, J. C. S., and Yates, J. T., Jr., *Langmuir* **8**, 1676 (1992).
17. Basu, P., Ballinger, T. H., and Yates, J. T., Jr., *Rev. Sci. Instrum.* **59**, 1321 (1988).
18. Sheppard, N., and Nguyen, T. T., *in* "Advances in Infrared and Raman Spectroscopy" (R. Clark and R. E. Hester, Eds.), Vol. 5. Heyden, London, 1978.
19. Hair, M. L., "Infrared Spectroscopy in Surface Chemistry." Dekker, New York, 1967.
20. Pimentel, G. C., and McClellan, A. L., "The Hydrogen Bond." Freeman, San Francisco, 1960.
21. Herzberg, G., "Molecular Spectra and Molecular Structure: II Infrared and Raman Spectra of Polyatomic Molecules." Van Nostrand, New York, 1945.
22. Zaera, F., Hoffman, H., and Griffiths, P. R., *J. Electron Spectrosc. Relat. Phenom.* **54/55**, 705 (1990).
23. Shimanouchi, T., "Tables of Molecular Vibrational Frequencies," National Standard Reference Data Series, NBS (US) 1962.
24. The apparent loss of CH_3Cl in the difference spectrum of pure SiO_2 may be a result of the fact that the difference spectrum was taken by comparing a spectrum recorded at 473 K to a spectrum recorded at 300 K.
25. Ho, W., *in* "Desorption Induced by Electronic Transitions, DIET IV" (G. Betz and P. Varga, Eds.), p. 48. Springer-Verlag, Berlin, 1990; and references therein.
26. Polanyi, J. C., and Rieley, H., *in* "Dynamics of Gas–Surface Interactions" (C. T. Rettner and M. N. R. Ashfold, Eds.), p. 329. Royal Society of Chemistry, Cambridge, 1991; and references therein.
27. Hoffman, M. R., Martin, S. T., Choi, W., and Bahnemann, D. W., *Chem. Rev.* **95**, 69 (1995).

28. Bohren, C. F., and Huffman, D. R., "Absorption and Scattering of Light by Small Particles," Wiley, New York, 1983.
29. Calvert, J. G., and Pitts, J. N. Jr., "Photochemistry." Wiley–Interscience, New York, 1966.
30. Greenler, R. G., Snider, D. R., Witt, D., and Sorbello, R. S., *Surf. Sci.,* **118**, 415 (1982).
31. Morrow, B. A., *Can. J. Che.* **48**, 2192 (1970).
32. Zaera, F., *Surf. Sci.* **262**, 335 (1992).
33. Fung, S. C., and Sinfelt, J. H., *J. Catal.* **103**, 220 (1987).
34. Anderson, J. R., and McConkey, B.H., *J. Catal.* **11**, 54 (1968).
35. Rasko, J., Bontovics, J., and Solymosi, F., *J. Catal.* **143**, 138 (1993).
36. Erley, W., *Surf. Sci.* **94**, 281 (1980).
37. Jo, S. K., and White, J. M., *Surf. Sci.* **261**, 111 (1992).
38. Weast, R. C. (Ed.), "CRC Handbook of Chemistry and Physics." CRC Press, Boca Raton, FL, 1991.
39. Zaera, F., *J. Phys. Chem.* **94**, 5090 (1990).